Experimental Validation of a Robotic Comanipulation and Telemanipulation System for Retinal Surgery

A. Gijbels, E.B. Vander Poorten, B. Gorissen, A. Devreker, P. Stalmans, D. Reynaerts

***Abstract*— Retinal Vein Occlusion is a common retinal vascular disorder which can cause severe loss of vision. Retinal vein cannulation is a promising treatment, but given the small diameter of retinal veins and the surgeon's limited positioning precision, it is considered too risky to perform this procedure manually. The authors previously reported on the development of both a robotic comanipulation and telemanipulation system which have the potential to augment the surgeon's positioning precision. This work investigates the potential benefit of these systems for retinal surgery. For this purpose, a targeting test setup was developed to quantify the attainable positioning precision one can expect when using the robotic systems during procedures like retinal vein cannulation. Ten subjects completed targeting tests in a free-hand, comanipulation and telemanipulation fashion. Results show that both the usage of the comanipulation and telemanipulation system significantly improve the positioning precision compared to a free-hand test. The telemanipulation system currently outperforms the comanipulation system with respect to precision, while subjects appreciate the remarkable ease of use of the comanipulation system.**

I. Introduction

A. Retinal Vein Occlusion and Retinal Vein Cannulation

Retinal surgery is considered as an extremely challenging type of surgery because of the scale and the fragility of the retinal anatomy. For some diseases, such as Retinal Vein Occlusion (RVO), the most promising procedure is even too difficult and risky to perform, forcing the surgeons to rely on less effective procedures. RVO is an eye condition which affects an estimated 16.4 million people worldwide [1]. It is the second most common retinal vascular disorder after diabetic retinal disease. The disease occurs when a clot is formed in a retinal vein (Fig. 1). This causes the patient to slowly lose his/her sight. Today, there is no proven effective treatment clinically available for this disease [2]. A promising treatment is retinal vein cannulation (Fig. 1). During this procedure, the surgeon's objective is to inject an adequate dose of t-Pa, a clot-dissolving agent, directly into the occluded retinal vein. A surgical microscope is placed above the patient's eye in order to have visual feedback on the surgical scene. Several research groups previously reported on successful cannulations in animal and human models [3], [4]. However, due to safety issues, the procedure is not performed clinically today. The needle must be inserted in a fragile vein with a diameter of only 400 µm or smaller

Andy Gijbels, Emmanuel Benjamin Vander Poorten, Benjamin Gorissen, Alain Devreker and Dominiek Reynaerts are with the Department of Mechanical Engineering, University of Leuven, 3001 Heverlee, Belgium

Peter Stalmans is with the Department of Ophthalmology, University of Leuven, 3000 Leuven, Belgium

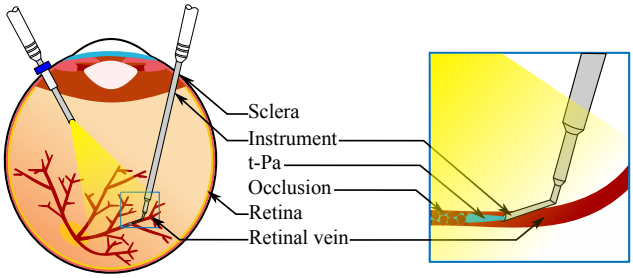

Fig. 1. Retinal Vein Cannulation: a hollow needle is inserted through the sclera and used to inject a clot-dissolving agent into an occluded vein which is causing RVO.

[5] and kept there for several minutes before the fluid is fully injected. Two types of unintended motions make it extremely difficult to correctly insert and to keep the tip of the needle inside the vein. First, surgeons suffer from physiological hand tremor. Because of this the tip of the needle vibrates with an rms amplitude in the order of 180 µm [6]. Second, the eye will rotate during the procedure when lateral forces are applied on the incision with the instrument. These rotations cause the retina to move, which forces the surgeon to aim at a dynamic target. These issues motivate the use of robotic assistance to perform retinal procedures like retinal vein cannulation.

B. Robotic-assisted retinal surgery

A fair number of robotic systems for retinal surgery have been reported in literature. A hand-held device capable of limited motion scaling and actively reducing tremor was developed at Carnegie Mellon University [7]. Researchers at Johns Hopkins University introduced a comanipulation strategy for retinal surgery [8]. Here, the surgeon shares control over the instrument with a robotic arm which task is to filter tremor and limit the instrument speed. The first telemanipulation system designed for eye surgery was developed at the California Institute of Technology [9]. Benefits of such a system like motion scaling and improved ergonomics for the surgeon motivate the usage of such a system. Other examples of robotic systems designed for retinal surgery are described in [10]–[13].

The authors previously reported on the development of a robotic comanipulation system [14] and a telemanipulation system [15] for retinal surgery. This work reports on an experimental campaign to evaluate the performance of these systems. First, the components and functionalities of the devices are briefly reviewed. Second, the development of

a targeting test setup used for the experimental campaign is discussed. Ten persons conducted targeting tests on this setup in a free-hand, comanipulation and telemanipulation fashion. The test protocol and results are discussed in detail.

II. Components and Functionalities of the Developed Robotic Systems

Figure 2 depicts the developed robotic comanipulation and telemanipulation system and other equipment that is being used. The comanipulation system consists of the surgical manipulator and two foot switches (not on the figure). The telemanipulation system additionally consists of the haptic joystick.

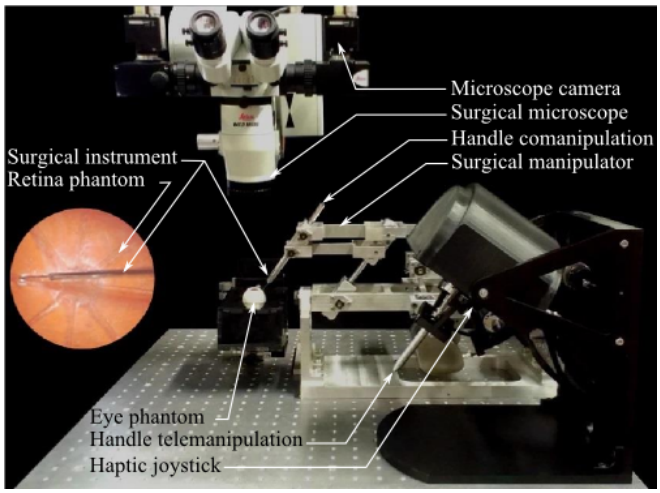

Fig. 2. Overview on the developed robotic systems and other equipment.

A. The comanipulation system

The instrument is attached to the surgical manipulator. The surgeon co-operatively moves (comanipulates) the instrument by directly gripping and manipulating the instrument. During this process the manipulator influences the instrument's motion in two ways. First, it limits the degrees of freedom (DOFs) of the instrument from six to four (Fig. 3(a)). These are two rotations θ and ϕ about the incision, a rotation ψ about the instrument axis and a translation R along the direction of the instrument axis and through the incision. The two translational DOFs in the plane tangential to the sclera are eliminated to prevent unwanted eye rotations and thus movements of the retina during the procedure. The four DOFs are implemented mechanically by virtue of a Remote Center of Motion (RCM) mechanism of which the RCM is aligned with the incision using an XYZ-stage [14]. Second, the surgeon can alter the system's resistance to instrument motions in the four DOFs using the foot pedals. The resistance is applied by four brushed DC motors. Both the type, i.e. viscous damping or blocking, and the level of motion resistance can be tailored to the surgical phase at hand. Three phases mostly characterize a retinal vein cannulation: approach, insertion and injection (Fig. 4). During the approach phase the surgeon enters the eye with the needle via the sclera and crosses

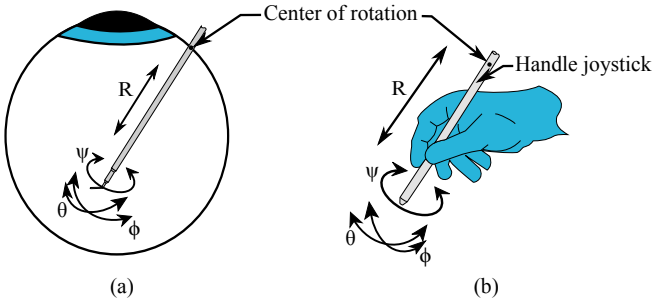

Fig. 3. (a) The four DOFs implemented in the surgical manipulator. (a)+(b) Spherical mapping in the telemanipulation system of the pose of the handle of the haptic joystick onto the pose of the instrument.

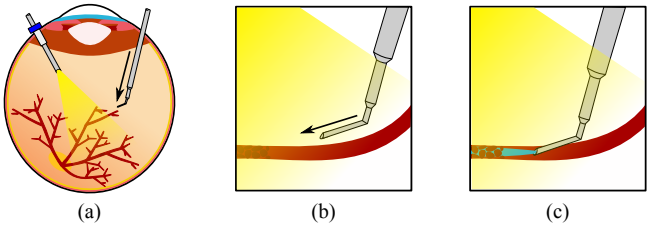

Fig. 4. Three phases mostly characterize a retinal vein cannulation: (a) approach, (b) insertion and (c) injection. The comanipulation and telemanipulation controllers provide task-dependent support.

the inner side of the eye to reach the occluded vein. Since this a relatively long distance to cover and no precision is required here, no motion resistance is needed. During the insertion phase the needle is carefully introduced into the occluded vein. The system assists the surgeon during this phase by viscously damping the instrument's motion. The damping filters the surgeon's tremor and also slows down the intended movements facilitating a slow and precise approach of the vein. During the injection phase, the needle tip must be kept immobile inside the vein. This is done by blocking the system and corresponding the instrument. When the injection is completed, the surgeon gently retracts the needle from the vein and the eye. Similar types and levels of motion resistance are used for the latter phases and for the insertion and approach phase respectively. At all times, the operator can increase the level of viscous damping by pressing an incremental foot switch. In addition the operator can lock the system by pressing a death-man's foot switch. Since the surgical manipulator is fully back-drivable and mechanically gravity compensated, these functionalities are implemented using a basic position/angle-to-force/torque lead controller for every DOF [14]. The maximum damping coefficients for each DOF are set to: $c_R = 400$ Ns/m, $C_\theta = 2$ Nms/rad, $C_\phi = 2$ Nms/rad and $C_\psi = 0.2$ Nms/rad. Instabilities occur when higher damping coefficients are used. Although, the coefficients are assumed to be sufficient to enable a proper positioning ability.

B. The telemanipulation system

When using the telemanipulation system, the instrument is attached to the same surgical manipulator that is used for the comanipulation system, here thus acting as a robotic

slave. The surgeon manipulates the handle of a 4-DOF spherical haptic joystick that takes the role as a master input device. The pose of the handle is mapped onto the pose of the instrument (Fig. 3). In this way, the motion inversion between the tool handle and the instrument, which is common to retinal surgery, is eliminated. Instead of virtual damping, the telemanipulation system allows the use of motion scaling to slow down intended movements and to reduce tremor. The surgeon can gradually increase the level of scaling by pressing the incremental foot switch. For a retinal vein cannulation typically no scaling is applied during the approach phase while higher scale factors are used during the insertion phase. A dead-man's foot switch is programmed to decouple the surgical manipulator from the joystick. This decoupling functionality has a double purpose. First, it is used to immobilize the surgical manipulator during the injection phase. The manipulator will maintain its pose at the moment of pressing the pedal. Second, when high scale factors are used, the joystick easily reaches the workspace boundaries. In such case, the operator must reset the mapping between the master and slave to be able to continue moving on the intended path. By pressing the dead-man's foot switch the operator can reposition the joystick handle while the surgical manipulator remains stationary. The surgeon could also use this clutching functionality to realign the joystick handle with the instrument when a mismatch in orientation between the two is perceived as being non-intuitive. Currently, the actuators of the joystick are solely used for gravity compensation. The surgical manipulator uses a position/angle-to-force/torque lead controller in every DOF to follow the pose reference given by the joystick. The controller stiffness's for each DOF are set to: $k_R = 2500$ N/m, $K_\theta = 20$ Nm/rad, $K_\phi = 20$ Nm/rad and $K_\psi = 20$ Nm/rad. These stiffness values are sufficient to avoid any noticeable lag between the master and slave motions. The maximum scale factor for each DOF is set to 5. During preliminary experiments, subjects considered this an adequate level of scaling for a proper positioning ability.

III. Development of a targeting test setup

This section describes the development of the test device that was used to conduct positioning experiments. The purpose of conducting targeting experiments is threefold. First, such tests help quantifying the attainable positioning precision during positioning tasks on the retina and the potential benefit of using robotic assistance for this task. Second it becomes possible to investigate how people use and exploit the different features provided by the developed assistive devices. Third, it allows to gather subjective feedback to acquire a better understanding of the user's appreciation of these systems, which gives us the opportunity to further optimize the operation quality prior to moving to more realistic animal or human models.

The test device is designed to automatically register the performance of people hitting targets with a needle. The performance is measured as the time needed to successfully hit a target and the number of positioning errors made in the process.

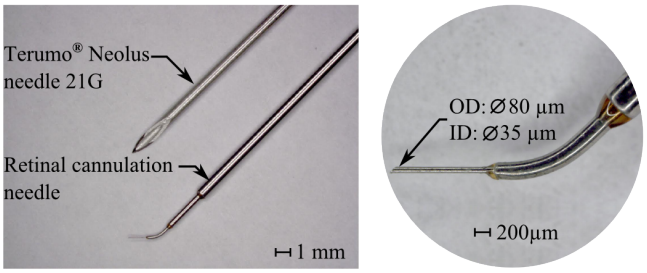

Fig. 5. (a) A standard 21G Terumo Neolus needle and a needle developed specifically for performing a retinal vein cannulation. b) Detail of the tip of the developed needle.

A. Determining the target size

Retinal veins have a diameter up to 400 µm [5]. Glass micro pipettes with an outer tip diameter of 20 µm have been used for experimental retinal cannulations [16]. Though, the use of stainless steel needles is advised because of the fragility of glass micro pipettes. By the author's knowledge, the authors developed the most slender stainless steel needle that is suited for retinal cannulations (Fig. 5). The outer and inner tip diameter of this needle are 80 µm and 35 µm respectively. In this case, a minimum positioning precision of 320 µm is required to successfully insert the needle into the largest vein. The robotic systems are designed to enable a positioning precision of 10 µm. Therefore, the positioning ability is tested using targets ranging from 10 µm to 320 µm. Fitts' law is used to determine appropriate target sizes within this range. According to this law, a logarithmic relationship exists between the time T to hit a target and the ratio of the distance D from the start position to the target and the width W of the target [17]:

$$T = a + b.log_2(\frac{D}{W} + 1). \quad (1)$$

The constants a and b depend on the user and on the used positioning device or method. The logarithmic part in this equation is called the index of difficulty ID. For this test setup, six targets are chosen with a width ranging from 10 µm to 320 µm and with a linearly decreasing ID. Given the number of targets and the width of the thinnest target W_1 and the thickest target W_N, the target sizes W_i can be calculated:

$$W_i = W_1 \lambda^{\frac{log_\lambda(W_N/W_1)i-1}{N-1}} \quad i = 1..N \quad \lambda \in \mathbb{R}^+ \setminus \{1\}. \quad (2)$$

The resulting target widths are then: 10 µm, 20 µm, 40 µm, 80 µm, 160 µm and 320 µm. A standard and quite robust 21G Terumo Neolus needle (Fig. 5(a)), which has a tip radius of only 1.5 µm, is used to minimize the influence of the needle on the required positioning precision to hit a target.

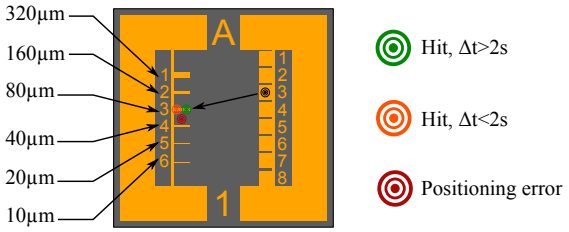

Fig. 6. The test plate consists of targets with a width ranging from 10 µm to 320 µm at the left-hand side. For every target a corresponding start position at the right-hand side exists. The test person is asked to first hit the start position and then to hit the target for two uninterrupted seconds. Hitting the target for less than two seconds or missing the target is considered as an error.

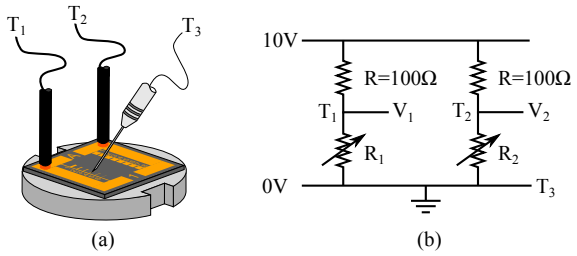

Fig. 7. (a) Terminals T_1, T_2 and T_3 are connected to the targets, the start positions and the needle respectively. (b) An electrical circuit enables the registration of the type of contact made with the needle by measuring the voltages at T_1 and T_2. Four contact types can be distinguished: target, start position, silicon and no contact.

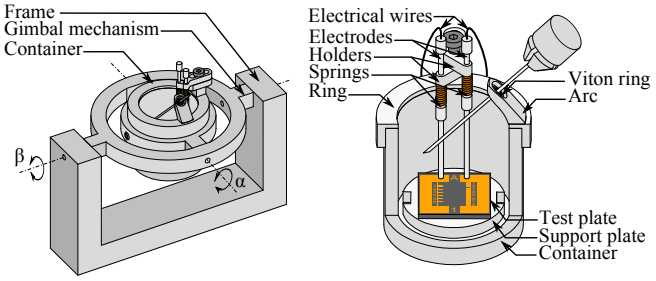

Fig. 8. Design of the test plate holder. The test plate is fixed on top of a support plate and placed inside a cylindrical container. The container is supported by a gimbal mechanism which enables it to rotate in two DOFs. Rigid electrodes are used to connect the test plate with the electrical wires of the acquisition system.

B. Design test plate

A test plate is designed to enable an automated registration of the subject's targeting performance during the experiment. The six targets are patterned as lines with a width W onto a single plate (Fig. 6). For each target on the left a separate start position exists on the right. Since only the effect of the target width on the performance is of interest in this test, the corresponding start positions and targets are chosen to be equidistant (distance is set to 5 mm). Furthermore, in order to avoid the effect of motion along preferential directions, the trajectory from start to end position is made so that each time a combined motion in R, θ and ϕ is required to approach a target. Note that the use of the ψ-DOF is omitted in this test since the used Terumo Neolus is roughly speaking an axisymmetric needle. An electrical circuit is designed to register and differentiate between contacts with a start position, a target and any other location on the plate (Fig. 7). The start positions and targets are patterned with gold onto a silicon plate and are wired to terminals T_1 and T_2 respectively. T_1 and T_2 are connected to a voltage source of 10 V via a resistor of 100 Ω. The needle is wired to terminal T_3, which is grounded. The resistances R_1 and R_2 between T_1 and T_3 and T_2 and T_3 respectively depend on the material being touched with the needle. Gold, silicon and air respectively have a low, intermediate and high electrical resistivity. Given this difference in resistivity and the two voltage dividers present in the electrical circuit, the type of contact can be registered by measuring voltages V_1 and V_2 at terminals T_1 and T_2 respectively. The silicon test plate is patterned with a layer of gold with a thickness of 250 nm using photolithography.

C. Design test plate holder

As explained earlier, one of the advantages of the surgical manipulator is that it eliminates unwanted eye rotations common to conventional retinal surgery. To include this complexity into the experiment a test plate holder was designed to simulate the mobility of the eye during the experiments (Fig. 8). The test plate is carefully fixed on an aluminium support plate using wax. This keeps the brittle object from breaking while assuring it can easily be replaced using a heat source. The test plate is placed inside a cylindrical container. The container is supported by a passive gimbal mechanism such that it can freely rotate about two perpendicular axes α and β. A ring with an arc is mounted on top of the container. The arc consists of a hole which is equipped with an O-ring. The O-ring simulates the incision into the eye through which the instrument accesses the inner part of the eye. The dimensions of the container and the position of the O-ring closely correspond to those of a human eye and of the incision made during retinal surgery. Rigid electrodes are used to connect the start positions and the targets with the electrical wires of the acquisition system. Movable electrode holders are used to correctly position the electrodes with respect to the test plate. Springs guarantee the contact between the electrodes and the test plate. Figure 9 visualizes the test setup and an example of a test plate that is fixed on a support plate.

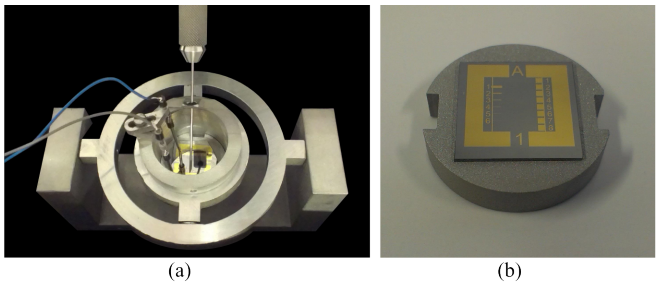

Fig. 9. (a) The developed test setup (b) Example of a test plate that is fixed on a support plate.

IV. Experiments

Ten right-handed subjects took part in the experimental campaign. They have no experience in surgery and variable experience with the use of joysticks or simulators and tasks requiring precision handling. This section discusses the protocol and gives an overview on the results of the experiments.

A. Protocol

The goal of the targeting test is to hit each target for two uninterrupted seconds and as fast as possible, but with a minimum number of positioning errors and failed hits (Fig. 6). For this experiment, a *positioning error* is defined as touching the silicon and thus missing the target. A *failed hit* is defined as touching the target for less than two uninterrupted seconds. The duration of two seconds to classify a hit as being successful was chosen in order to exclude lucky hits. For a specific target, the registration of the time and the counting of the number of positioning errors and failed hits starts when the needle departs from the corresponding start position. Targets are presented in a random order. During the experiment, the subject receives visual feedback from a stereoscopic microscope and auditive computer-generated feedback through a pair of headphones. When gold is touched, a continuous beep sound is generated. When the silicon is touched, an alternating beep sound is produced. In the latter case, the subject retracts the instrument from the test plate before reapproaching the target. This keeps the subjects from simply sliding over the test plate until contact with the target is being made. When a target is successfully hit, the next target number is automatically announced. The subjects are asked to perform the targeting test in three operation modes: free-hand, via the comanipulation system and by using the telemanipulation system. The order in which these modes are used is randomized as well. For every operation mode three sets of all six targets are recorded after a learning exercise of two sets is conducted. During the test, an observer explains the protocol, demonstrates each operation mode and intervenes in the event of anomalies. The experiment itself is fully automated to avoid any human errors which could make the test invalid. The observer has visual feedback on the test plate by looking at a camera live stream of the test plate on a computer screen and auditive feedback using an extra pair of headphones. After the experiment, the subjects are asked to fill in a questionnaire consisting of 21 statements about the experiment and the different operation modes. Answers are given using a five-level Likert scale and text boxes can be used for detailed statements.

B. Results

Figure 10 shows bar charts which depict the mean and standard deviation of the time to successfully hit a target, the number of positioning errors and the number of failed hits as a function of the target width and the operation mode. These graphs are derived from the thirty data points measured for each target width and operation mode. A data point in a data set is considered as an outlier when it is located outside 1.5 times the interquartile range above the upper quartile and below the lower quartile of the data set. Based on this criterion, a maximum number of five outliers was detected and removed in all data sets. Levene's test and Welch's t-test are used to assess the equality of variances and means respectively of the three operation modes for the three metrics and the six targets. Welch's t-test is used instead of the more conservative Student's t-test since most data sets appear to have unequal variances. In the following, means and variances between two modes are considered as being significantly different when p-values smaller than 0.05 are calculated. Figure 11 depicts a performance chart of a subject who carried out the experiment in a manner which is representative for the overall population. It depicts the start and end time of positioning errors, failed hits and the successful hit for each target and operation mode. Also the level of damping and scaling that the user applied as function of time and the start and end time of clutching are depicted. Table I depicts the most informative questions and answers taken from the questionnaire.

V. Discussion

Figure 10(b) and 10(c) and the conducted statistical analysis show that the average number of positioning errors and failed hits for the five smallest targets are significantly higher for the free-hand mode. As expected, the differences are more explicit for smaller targets. In the questionnaire, people indicate that their poor results for this mode are mainly due to tremor. Container rotations are considered less of a problem, though most people appreciate the immobilized incision point when using robotic assistance. Furthermore, the bar charts indicate significantly larger differences in performance among subjects in free-hand mode compared to the robotic modes. This can be explained by the significant different levels of tremor among subjects, which could even be observed visually. The subjects and the results point out that both damping and scaling reduce tremor and thus, as expected, are helpful to correctly hit the targets. Nevertheless, the number of failed hits is significantly higher for the comanipulation mode compared to the telemanipulation mode for the 10 μm-, 20 μm- and 40 μm-target. Failed hits start appearing at 40 μm and 10 μm for the comanipulation and telemanipulation mode respectively. Some subjects mentioned that they would benefit from higher levels of damping in order to hit the smallest targets in a single attempt. Low levels of tremor caused subjects to lose grip on these targets in this mode. On the contrary, most people agree that the maximum level of scaling of the telemanipulation system is sufficient. Some people point out that for this mode positioning errors solely originate from difficulties in clearly seeing the smallest targets. They further mention that with better vision they would be able to hit each target in a single attempt using the telemanipulation mode. Despite the currently superior positioning precision of the telemanipulation system, people generally do not agree on the system's ease of use. First, mismatches between the orientation of the joystick handle and the needle are perceived as non-

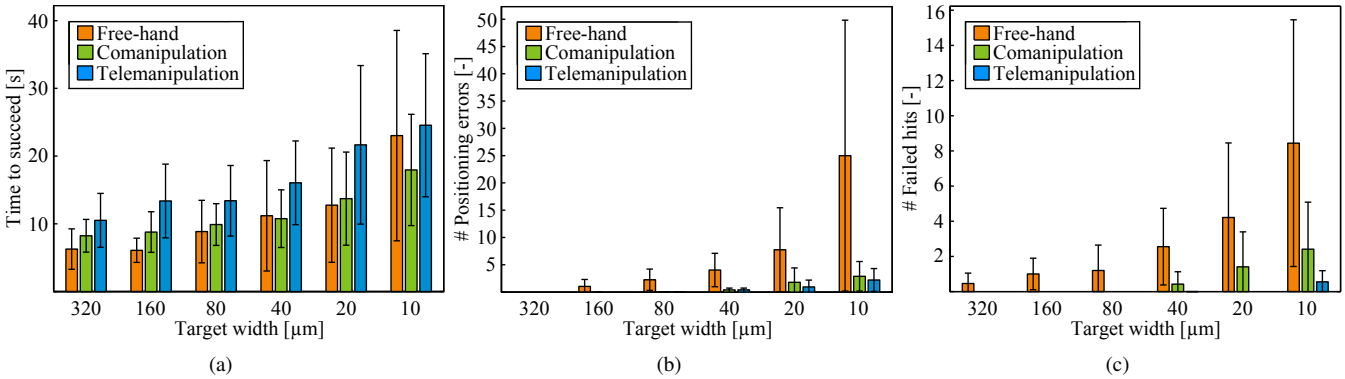

Fig. 10. Bar charts depicting the mean and standard deviation of (a) the time to successfully hit a target, (b) the number of positioning errors and (c) the number of failed hits as a function of the target width and the operation mode.

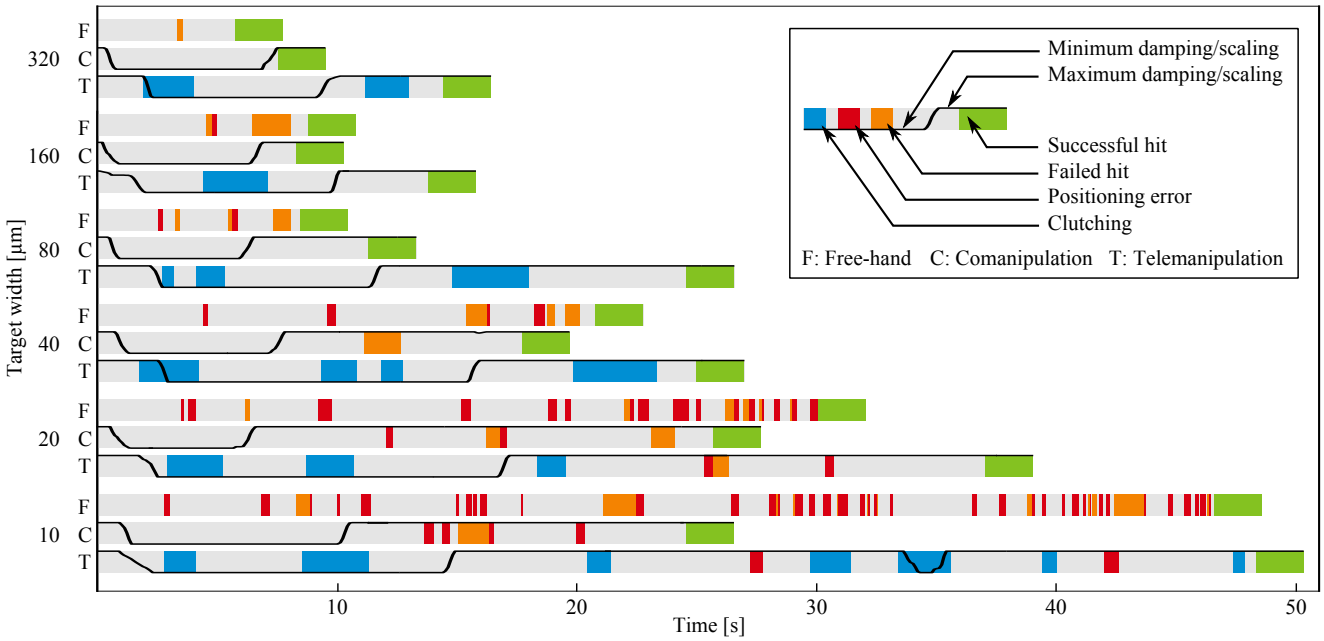

Fig. 11. Performance chart of a subject representative for the population. It depicts the start and end time of positioning errors, failed hits and the successful hit for each target and operation mode. Also the level of damping and scaling over time and the start and end time of clutching are depicted.

TABLE I

SELECTION OF THE MOST INTERESTING QUESTIONS AND ANSWERS TAKEN FROM THE QUESTIONNAIRE.

Questions	Strongly disagree	Disagree	Nor agree or disagree	Agree	Strongly agree
Free-hand					
1. Hitting the targets correctly is difficult.	0	0	2	5	3
2. Container rotations make it difficult to correctly hit the targets.	0	0	5	3	2
3. Needle vibrations make it difficult to correctly hit the targets.	0	0	0	8	2
Comanipulation					
1. Hitting the targets correctly is difficult.	3	4	3	0	0
2. The system is easy to use.	0	0	1	4	5
3. The damping is helpful to correctly hit the targets.	0	0	0	3	7
4. The maximum level of damping is sufficient.	0	2	3	4	1
5. The inverse motion between the handle and the needle is confusing.	8	1	0	1	0
Telemanipulation					
1. Hitting the targets correctly is difficult.	3	4	3	0	0
2. The system is easy to use.	0	3	4	3	0
3. The scaling is helpful to correctly hit the targets.	0	1	1	1	7
4. The maximum level of scaling is sufficient.	0	0	2	2	6
5. Unequal orientations of the handle and the needle are confusing.	1	3	1	5	0
6. The clutching procedure is intuitive.	0	4	3	2	1

intuitive. Second, the clutching procedure necessary in the event of such mismatches or when reaching the workspace boundaries of the joystick, is experienced as being somewhat cumbersome. The performance chart shows repositioning periods up to three seconds. This explains the significantly longer period necessary to successfully hit a target compared to the comanipulation mode, which doesn't require any clutching (Fig. 10(a)). Further, most people didn't perceive the inverse motion between handle and needle in case of the comanipulation mode as confusing. As a consequence the elimination of the inverse motion in the telemanipulation system was not perceived as a benefit. Based on these considerations, eight people preferred using the comanipulation system instead of the telemanipulation system. Four people even noted they would rather do another test in free-hand mode than in telemanipulation mode. Note, that in general the positioning times in free-hand mode are significantly shorter than for the telemanipulation mode. This is because in free-hand mode it takes less time to cover the distance D to the target. It should be noted that more extensive training with the telemanipulation system could solve this problem. On the contrary, the differences in positioning time between the free-hand and comanipulation mode are insignificant for targets ranging from 80 μm to 10 μm. The benefit of using a telemanipulation system rather than using a comanipulation system with adequate levels of damping is not demonstrated. If any, these benefits should weigh up against the added complexity, cost and changes in the conventional work flow. Finally, investigations on all performance charts show that most people either press the pedal fully or do not press the pedal at all to control the level of damping and scaling (Fig. 11). Levelling the incremental pedal at intermediate positions is considered as tiring. Furthermore, six people note that being able to turn the damping of the comanipulation system on and off would be sufficient, while the other four people would even appreciate a fixed level of damping. On the contrary, six people require the telemanipulation system to have multiple levels of scaling, while only four people consider being able to turn the scaling on and off as sufficient. Fixed and high scaling is undesirable since it requires frequent application of the clutching procedure.

VI. Conclusion and Future work

This work reported on user experiments to investigate the potential benefit of the developed comanipulation and telemanipulation system for retinal surgery. A targeting test was developed to quantify the attainable positioning precision during precision tasks on the retina. The user's performance, use of the different features provided by the robotic devices and subjective feedback on the systems was investigated and discussed. Results show that both the usage of the comanipulation and telemanipulation system significantly improve the positioning precision with respect to the free-hand mode. The highest positioning precision was recorded in the telemanipulation mode. An inadequate maximum level of damping clarifies why in comanipulation mode people fail to reach the same positioning precision as in the telemanipulation mode. In general, people prefer using the comanipulation system because it significantly improves the positioning precision compared to the free-hand mode, while it is easier to use than the telemanipulation system. The maximum level of damping can be further increased to optimize the performance of the comanipulation system.

VII. Acknowledgments

The authors would like to thank warmly all the people who participated in the experiments. This work was supported by an FP7-People Marie Curie Reintegration Grant, PIRG03-2008-231045 and by a PhD grant from the Institute for the Promotion of Innovation through Science and Technology in Flanders (I.W.T.-Vlaanderen), 101445.

References

[1] R. Sophie, "The prevalence of retinal vein occlusion: Pooled data from population studies from the united states, europe, asia, and australia," *Ophthalmology*, vol. 117, pp. 313– 319, 2010.

[2] B. Nilufer and B. Cosar, "Surgical treatment of central retinal vein occlusion," *Acta Ophthalmologica*, vol. 86, pp. 245–252, 2008.

[3] J. Weiss and L. Bynoe, "Injection of tissue plasminogen activator into a branch retinal vein in eyes with central retinal vein occlusion," *Ophthalmology*, vol. 108-12, pp. 2249–2257, 2001.

[4] L. A. Bynoe, R. K. Hutchins, H. S. Lazarus, and M. A. Friedberg, "Retinal endovascular surgery for central retinal vein occlusion: Initial experience of four surgeons," *Retina*, vol. 25, pp. 625–32, 2005.

[5] F. Skovborg, V. Nielsen, E. Lauritzen, and O. Hartkopp, "Diameters of the retinal vessels in diabetic and normal subjects," *Diabetes*, vol. 18(5), pp. 292–298, 1969.

[6] C. N. Riviere and P. S. Jensen, "A study of instrument motion in retinal microsurgery," in *Conf. IEEE Eng. Med. Biol. Soc*, pp. 59–60, 2000.

[7] S. Yang, R. A. MacLachlan, and C. N. Riviere, "Design and analysis of 6 dof handheld micromanipulator," *Proc. IEEE Int. Conf. on Robotics and Automation (ICRA).*, pp. 1946 – 1951, 2012.

[8] A. Uneri, M. Balicki, J. Handa, P. Gehlbach, R. Taylor, and I. Iordachita, "New steady-hand eye robot with microforce sensing for vitreoretinal surgery research," *Int. Conf. on Biomedical Robotics and Biomechatronics*, pp. 814–819, 2010.

[9] S. Charles, H. Das, T. Ohm, C. Boswell, G. Rodriguez, R. Steele, and D. Istrate, "Dexterity-enhanced telerobotic microsurgery," *Proc. of the IEEE Int. Conf on Advanced Robotics*, pp. 5–10, 1997.

[10] W. Wei, R. Goldman, N. Simaan, H. Fine, and S. Chang, "Design and theoretical evaluation of micro-surgical manipulators for orbital manipulation and intraocular dexterity," *ICRA*, pp. 3389–3395, 2007.

[11] A. Guerrouad and P. Vidal, "Smos: Stereotaxical microtelemanipulator for ocular surgery.," *Medicine and Biology Society*, pp. 879–880, 1989.

[12] H. Meenink, R. Hendrix, P. Rosielle, M. Steinbuch, and M. de Smet, "A master-slave robot for vitreo-retinal eye surgery," *Proc. of the 10th Int. Conf. of European Society for Precision Engineering and Nanotechnology*, 2010.

[13] M. Nasseri, M. Eder, S. Nair, E. Dean, M. Maier, D. Zapp, C. Lohmann, and A. Knoll, "The introduction of a new robot for assistance in ophthalmic surgery," *35th Annual Int. Conf. of the IEEE Engineering in Medicine and Biology Soc. (EMBC'13)*, 2013.

[14] A. Gijbels, N. Wouters, P. Stalmans, H. Van Brussel, D. Reynaerts, and E.B. Vander Poorten, "Design and realisation of a novel robotic manipulator for retinal surgery," *Proc. IEEE Int. Conf. on Intelligent Robots and Systems*, 2013.

[15] A. Gijbels., E.B. Vander Poorten, P. Stalmans, H. Van Brussel, and D. Reynaerts, "Design of a teleoperated robotic system for retinal surgery," *Proc. IEEE Int. Conf. on Robotics and Automation*, 2014.

[16] B. Mitchell, J. Koo, I. Iordachita, P. Kazanzides, A. Kapoor, J. Handa, G. Hager, and R. Taylor, "Development and application of a new steady-hand manipulator for retinal surgery," *Proc. IEEE Int. Conf. on Robotics and Automation (ICRA)*, pp. 623–629, 2007.

[17] P. Fitts, "The information capacity of human motor system in controlling the amplitude of movement," *Journal of Experimental Psychology*, vol. 47-6, pp. 381–391, 1954.